Bioorganic Chemistry 89 (2019) 102978

Contents lists available at ScienceDirect

Bioorganic Chemistry

journal homepage: www.elsevier.com/locate/bioorg

# Design and synthesis of new benzoxazole/benzothiazole-phthalimide hybrids as antitumor-apoptotic agents

John N. Philoppes, Phoebe F. Lamie

*Department of Pharmaceutical Organic Chemistry, Faculty of Pharmacy, Beni-Suef University, Beni-Suef 62514, Egypt*

ARTICLE INFO

*Keywords:*
Benzothiazole
Benzoxazole
Phthalimide
Antitumor
Synthesis

ABSTRACT

Herein, we synthesized a series of twelve benzoxazole and benzothiazole derivatives incorporated with phthalimide core as anticancer agents. The most active compounds were **5a** and **5g** against HepG2 and MCF7 cell lines with $IC_{50}$ = 0.011 and 0.006 μM, respectively.

They evaluated against EGFR and HER2 enzymes. From cell cycle analysis, it was observed that test compounds exerted pre G1 apoptosis and cell cycle arrest at G2/M phase. The achieved results suggested that apoptosis was due to activation of caspase-7 and caspase-9. EGFR was chosen as a biological target for carrying molecular modeling study for the newly synthesized compounds.

## 1. Introduction

Cancer is the second disease leading to death worldwide [1–3]. Hepatocellular carcinoma is one form of cancer originates in liver cells and leads to high mortality rates in the world today [4].

Due to cytotoxicity of most anticancer agents, researchers seek every day to develop more effective, selective and safe chemotherapeutic agents [2].

By searching the literature, we found that azo compounds such as benzoxazole and benzothiazole derivatives had different types of biological activities especially antitumor activity [5–10].

Moreover, a number of benzothiazole derivatives displayed good anticancer activity and apoptotic effect on HepG2 cells both *in-vitro* and *in-vivo* [11,12].

3′-Substituted 2-(4-aminophenyl)benzothiazoles represent an important class of antitumor agents by exhibiting inhibitory activity against certain cancer cell lines (e.g., breast MCF7, MDA 468; renal TK 10; overian IGROV) [13,14].

Structure-activity relationships for these compounds showed that substitution at 3′-position of phenyl ring with either alkyl ($CH_3$) or halogen (I, Br, Cl) groups increased the potency and *in-vitro* activity against tumor cell lines, ($IC_{50}$ < 0.0001 μM) with bromo- and iodo-analogues against MDA468 cell line [14,15].

3′-Substituted 2-(4-aminophenyl)benzothiazoles are characterized by a unique biphasic dose-response relationship in sensitive cell lines. Low nanomolar concentration of test compounds for cell death, followed by low micromolar concentration for proliferative response in second growth phase (SGP). This was attributed to inactivation of a metabolite to the bioactive enzyme cytochrome P450 (CYP)1A1 [16,17].

On the other hand, imide derivatives have broad spectrum of pharmacological activities such as anti-inflammatory, antiviral, antibacterial and antitumor [18].

As it is known, angiogenesis, the process by which new capillary blood vessels are formed, plays an important role in growth and maintenance of solid tumors. Therefore, angiogenesis has become an attractive area for approaching new therapeutic agents [19]. Thalidomide (NKTA) – a phthalimide derivative- was used as a sedative and hypnotic drug in 1960, but it was withdrawn from clinics due to its teratogenic disorders [20,21]. In earlier 1990, thalidomide was proved to be an anti-angeogenic agent and effective in treatment of different diseases such as inflammation, immunodeficiency syndrome (AIDS) and cancer. It acts by inhibiting the production of tumor necrosis factor alpha (TNF-α), interleukin-1b (IL-1b), IL-2, IL-4, IL-5, IL-6, IL-10 and interferon-ɤ (IFN-ɤ) [20–26].

It has been showed that variation in thalidomide structure could eliminate its side effects like teratogenicity, while still maintaining the promising anticancer activity. As a result, many thalidomide analogs have been developed such as lenalidomide (Revlimid™) and pomalidomide [27–29]. Merging both benzothiazole and phthalimide rings together in one compound as in cantharidin containing benzothiazole possessed antitumor properties in hepatocellular carcinoma, breast cancer and non-small cell lung carcinoma [19,25,30].

Keeping in mind the molecular pharmacophores outlined above and in continuation to our work in the field of designing and synthesis of anticancer agents [31–35], molecular hypridization between

*E-mail addresses:* john_philoppes@yahoo.com (J.N. Philoppes), feebi.lamey@pharm.bsu.edu.eg (P.F. Lamie).

https://doi.org/10.1016/j.bioorg.2019.102978
Received 29 December 2018; Received in revised form 5 May 2019; Accepted 7 May 2019
Available online 10 May 2019
0045-2068/ 

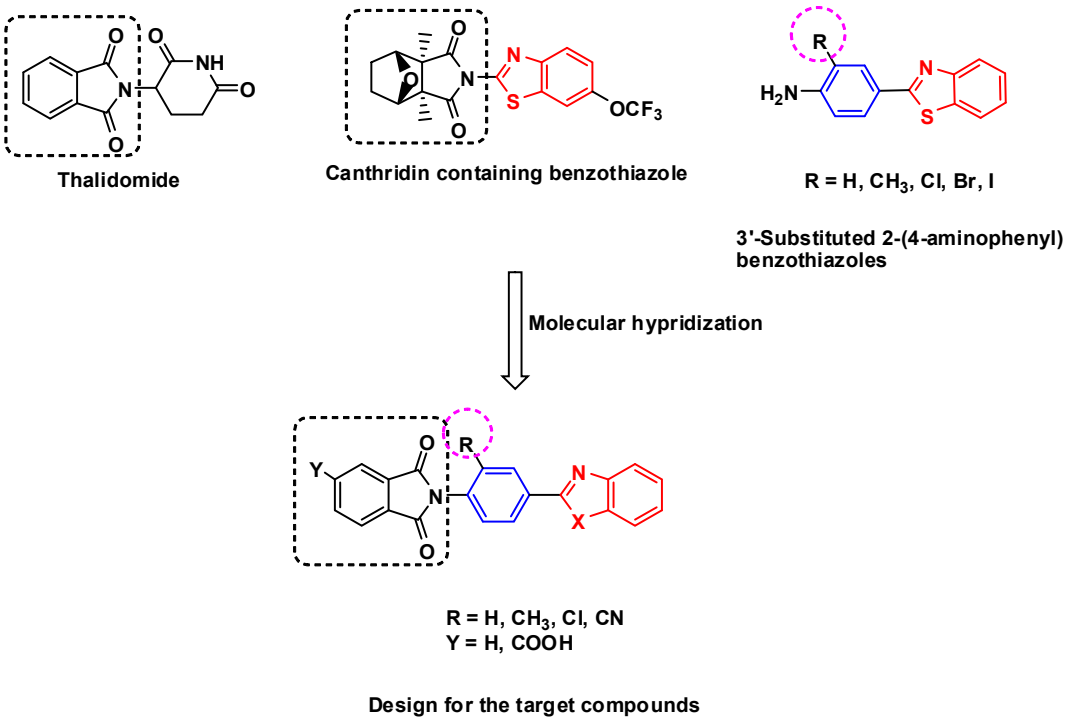


**Fig. 1.** Reported biologically active compounds and a design for the target compounds **5a–l**.

phthalimide ring and benzothiazole or its isoster benzoxazole nucleus has been designed and synthesized (Fig. 1). Their antitumor activity was evaluated against HepG2 and MCF7 cells. The most active derivatives were subjected to kinase enzyme activity determination on both EGFR and HER2 enzymes. Cell cycle analysis and apoptotic inducers activity were also parts of this study. Molecular docking study was performed for all the target compounds inside EGFR active site.

## 2. Results and discussion

### 2.1. Chemistry

The starting materials **1a&b**, **2a-d**, intermediates **3a–i, 4a&b**, and final target compounds **5a–l** were synthesized as shown in Scheme 1.

Cyclization of *o*-aminophenol **1a** or *o*-aminothiophenol **1b** with 4-aminobenzoic acid derivatives namely, 4-aminobenzoic acid,4-amino-3-methylbenzoic acid, 4-amino-3-cyanobenzoic acid and 4-amino-3-chlorobenzoic acid in polyphosphoric acid at a high temperature 180–220 °C resulted in the formation of 2-phenylbenzoxazole and 2-phenyl benzothiazole derivatives **3a–i** according to precautions of reported method [14,33].

Condensation of compounds **3a–i** with phthalic anhydride **4a** or phthalic anhydride-5-carboxylic acid derivative **4b** in glacial acetic acid afforded the target compounds **5a–l**.

IR spectra of **5a–l** showed the presence of two peaks for the two carbonyl groups of phthalimide part at the range 1786–1774 and 1734–1703 $cm^{-1}$. An additional C=O peak (COOH) in compounds **5d–f** and **5j–l** appeared at 1661–1687 $cm^{-1}$. Moreover, a dragged peak characterized for COOH group was observed in the later compounds at 3053–2543 $cm^{-1}$. Also, appearance of a peak due to CN group in **5b** and **5h** was observed at 2358 and 2234 $cm^{-1}$, respectively.

Moreover, $^1$HNMR spectra of **5a** and **5g** revealed the presence of a singlet signal at $\delta$ 2.24–2.28 ppm attributed to $CH_3$ protons, in addition to eleven aromatic protons in the range of aromatic region at $\delta$ 7.37–8.45 ppm.

A $D_2O$ exchangeable signal appeared in compounds **5d–f** and **5j–l** as a singlet signal due to COOH proton at $\delta$ 13.75 to 13.84 ppm.

### 2.2. Biological evaluation

#### 2.2.1. In-vitro antiproliferative activity

Twelve newly synthesized benzoxazole/benzothiazole phthalimide hybrids were tested through determination of their $IC_{50}$ values (half maximal inhibitory concentration) against two human cancer cell lines, liver HepG2, breast MCF7 and non-cancerous fibroblast cells (WI-38). The reference drugs used in this study were 5-flurouracil (5-FU) and erlotinib against HepG2 and MCF7, respectively.

The obtained *in-vitro* results were summarized in Table 1. Deep insight to the tabulated results showed that no cytotoxic activity was observed for targeted compounds on non-cancerous fibroblast cells (WI-38), ($IC_{50}$ = 28.82–122.31 μM). All the test compounds exhibited potent anticancer activity against HepG2 and MCF7 in nanomolar to micromolar range with $IC_{50}$ values between 0.011 and 0.036 μM and 0.006–0.468 μM, sequentially, except oxazole derivatives **5c**, **5d**, **5f** and thiazole derivative **5h** had $IC_{50}$ values 0.132–0.724 μM against HepG2 if compared to 5-FU (HepG2 reference) $IC_{50}$ = 0.034 μM.

Both benzoxazole and benzothiazole derivatives **5a**, **5b** and **5k** exhibited 1.7- to 3-folds more potent anticancer activity against HepG2 cell line than 5-FU, the reference drug. Moreover, compounds **5c** and **5g** were the most potent derivatives between the test compounds. They showed $IC_{50}$ values 9 and 6 nM with 79- and 118-folds more potent anticancer activity than erlotinib against MCF7 cell line.

The structure activity relationship revealed that the antiproliferative activity of the test compounds was in correlation with aryl and two heteroaryl rings of the hybride structure.

The presence of phthalimide ring in the structure of the test compounds resulted in the formation of a hydrogen bond between its C=O group and SH group of cysteine back bone amino acid of caspase-7 enzyme leading to induction of apoptosis [36].

Further analysis of the test compounds revealed that the presence of CN group in a hybrid structure of benzoxazole and phthalimide core **5b** led to increase activity against HepG2 cell line ($IC_{50}$ = 0.018 μM). Compounds bearing $CH_3$ group, benzoxazole and phthalimide **5a** or $CH_3$ group, benzothiazole and carboxy substituted phthalimide **5k** showed higher anticancer activity against HepG2 ($IC_{50}$ = 0.011 and

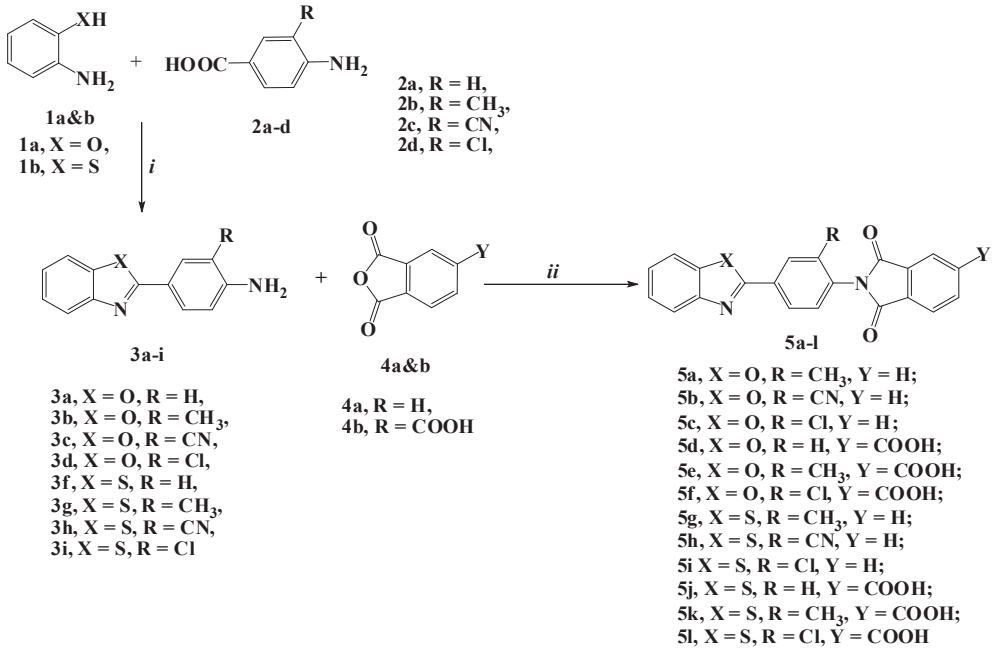


**Scheme 1.** Synthesis of the target compounds **5a–l**.

0.019 μM, respectively) if compared to 5-FU ($IC_{50}$ = 0.034 μM).

While, $CH_3$ group, benzoxazole and carboxy substituted phthalimide **5e** and $CH_3$ group, benzothiazole and unsubstituted phthalimide **5g** resulted in slight decrease in anticancer activity against HepG2 ($IC_{50}$ = 0.056 and 0.098 μM, sequentially) comparing to 5-FU.

Introduction of other groups such as Cl in benzoxazole analogues **5c**, **5f** and CN in **5h** showed marked decrease in activity ($IC_{50}$ = 0.132–0.724 μM). Also, the presence of benzoxazole and phenyl ring merged with carboxy substituted phthalimide **5d–5f** exhibited lower anticancer activity against HepG2 than benzothiazole analogues **5j–5l**.

On the other hand, unsubstituted phthalimide core gave better anticancer activity against MCF7 than phthalimide substituted with COOH group at 4-position.

Introducing Cl group **5c** ($IC_{50}$ = 0.009 μM) or $CH_3$ group **5g** ($IC_{50}$ = 0.006 μM) at phenyl ring with unsubstituted phthalimide core showed the highest anticancer activity against MCF7 cell line.

The presence of CN group at phenyl ring **5b** ($IC_{50}$ = 0.211 μM) and **5h** ($IC_{50}$ = 0.468 μM) resulted in slight decrease in antiproliferative activity between all the test compounds but still more active than the reference erlotinib ($IC_{50}$ = 0.71 μM).

Finally, we could conclude that benzoxazole and benzothiazole derivatives exerted a positive effect on the anticancer activity against MCF7 cell line. While, benzothiazole derivatives were more active than benzoxazole analogues against HepG2. The higher activity of most of the test compounds was observed in those bearing unsubstituted phthalimide core than carboxy substituted phthalimide ones.

The order of anticancer activity for the substituted groups at phenyl ring was, $CH_3$ > CN ≈ H > Cl against HepG2 cell line, while, $CH_3$ > Cl > H > CN against MCF7 cell line.

### 2.2.2. In-vitro enzyme inhibition assay

EGFR $IC_{50}$ for the most potent compounds **5a** and **5g** and the reference drug erlotinib was determined to be 0.23 and 0.35 μM relative to the reference erlotinib $IC_{50}$ = 0.15 μM, (Table 2). One further enzyme that is overexpressed in breast cancer, HER2 was used to help in exploring the mechanism of action of **5a** and **5g**. It was found that $IC_{50}$ values of **5a** and **5g** on HER2 were determined to be 0.45 and 0.33 μM, sequentially, (Table 2). From the tabulated results, it was observed that the most active antiproliferative compounds against HepG2 and MCF7 cell lines, **5a** and **5g**, demonstrated moderate effects against both kinases (EGFR and HER2) at 10 μM. The antiproliferative activity of the synthesized compounds might be due to apoptosis rather than tyrosin kinase inhibitory activity. Finally, we concluded that the mode of action for the synthesized compounds might be on those enzymes to some extent and further future studies should be considered to discover other enzymes participate in increasing the anticancer activity of the synthesized derivatives.

### 2.2.3. Caspase activation assay

Caspase-7 and caspase-9 are among caspases, a family of cysteine-aspartic protease enzymes which play important role in programmed cell death and can be used as indicators for induction of apoptosis by anticancer agents. Caspase-9 is an initiator caspase which initate the apoptosis signal while caspase-7 is one of executioner caspases which carry out the mass proteolysis that leads to apoptosis [37].

In this study, human liver HepG2 and breast MCF7 cell lines were treated with compounds **5a** ($IC_{50}$ = 0.011 μM) and **5g** ($IC_{50}$ = 0.006 μM), respectively, and protein expression levels of both caspase-7 and caspase-9 were determined in the treated cell lines. The obtained results showed significant over-expression in caspase-7 and caspase-9 protein level in treated samples (Table 3).

Thus, from above results, it was found that caspase-7 concentration for **5a/HepG2** and **5g/MCF7** was 1.449 ng/ml and 1.841 ng/ml, respectively. Moreover, concentration of caspase-9 for **5a/HepG2** and **5g/MCF7** was 22.72 ng/ml and 27.56 ng/ml, sequentially (Fig. 2).

These achieved results suggested that apoptosis was due to activation of caspase-7 and caspase-9.

### 2.2.4. Cell cycle analysis and apoptosis detection

Both HepG2 and MCF7 cell lines after treatment with the most potent compounds **5a** ($IC_{50}$ = 0.011 μM) and **5g** ($IC_{50}$ = 0.006 μM), sequentially was subjected to cell cycle analysis.

In both cell lines, HepG2 and MCF7 the percentages of cells in G0/G1 phase of the cell cycle were 55.37% and 48.92% and decreased to be 31.22% and 33.54% in G2/M phase for **5a** and **5g**, respectively (Figs. 3 and 4, Table 4).

Additionally, the percentage of apoptotic cells was increased from 1.65% in control untreated HepG2 to 21.25% in cells treated with 0.011 μM of compound **5a** (12-fold) and from 1.92% for control

**Table 1**
Cytotoxic activity ($IC_{50}$) for test compounds **5a–l** against HepG2, MCF7 and WI-38 cell lines.

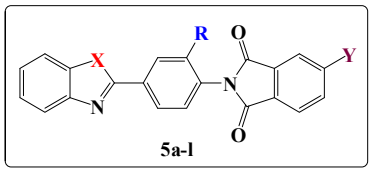


| Compound no. | Structure | | | *$IC_{50}$ results (μM) | | |
|---|---|---|---|---|---|---|
| | X | R | Y | HepG2 | MCF7 | WI-38 |
| **5a** | O | $CH_3$ | H | 0.011 | 0.024 | 97.06 |
| **5b** | O | CN | H | 0.018 | 0.211 | 84.11 |
| **5c** | O | Cl | H | 0.724 | 0.009 | 54.71 |
| **5d** | O | H | COOH | 0.326 | 0.02 | 122.31 |
| **5e** | O | $CH_3$ | COOH | 0.056 | 0.028 | 35.43 |
| **5f** | O | Cl | COOH | 0.132 | 0.019 | 38.33 |
| **5g** | S | $CH_3$ | H | 0.098 | 0.006 | 28.82 |
| **5h** | S | CN | H | 0.361 | 0.468 | 42.14 |
| **5i** | S | Cl | H | 0.036 | 0.014 | 31.04 |
| **5j** | S | H | COOH | 0.021 | 0.167 | 42.91 |
| **5k** | S | $CH_3$ | COOH | 0.019 | 0.013 | 45.94 |
| **5l** | S | Cl | COOH | 0.059 | 0.134 | 40.09 |
| **5-FU** | | | | 0.034 | -------- | -------- |
| **Erlotinib** | | | | --------- | 0.71 | -------- |

**Table 2**
$IC_{50}$ (μM) values of compounds **5a**, **5g** and erlotenib towards EGFR and HER2.

| Compound No. | $IC_{50}$ (μM) (EGFR) | $IC_{50}$ (μM) (HER2) |
|---|---|---|
| **5a** | 0.23 | 0.45 |
| **5g** | 0.35 | 0.33 |
| **Erlotenib** | 0.15 | 0.27 |

[a]Values are the mean of two independent replicates ± SD.

**Table 3**
Caspase-7 and caspase-9 concentrations in HepG2 and MCF7 cell lines treated with compounds **5a** and **5g** against control untreated cells.

| Compound | | Results | |
|---|---|---|---|
| Ser | Cpd. code. | Caspase-7 conc.ng/ml | Caspase-9 conc.ng/ml |
| 1 | **5a**/HepG2 | 1.449 | 22.72 |
| 2 | **5g**/MCF7 | 1.841 | 27.56 |
| 3 | cont.HepG2 | 0.3002 | 1.082 |
| 4 | cont.MCF7 | 0.1994 | 1.364 |

untreated MCF7 cells to be 18.26% when cells were treated with 0.006 μM of compound **5g** (9.5-fold), (Fig. 5).

From the above obtained results, the test compounds exerted pre G1 apoptosis and cell cycle arrest at G2/M phase.

### 2.2.5. *Evaluation of Bax and Bcl-2 expressions*

Pro-apoptotic protein Bax and anti-apoptotic protein Bcl-2 (B-cell lymphoma 2) expression levels were measured in both HepG2 cells treated with compound **5a** and MCF7 cells treated with compound **5g**. The obtained results showed up regulation in the apoptotic protein, Bax. On the other hand, it was found that the anti-apoptotic Bcl-2 protein expression was decreased (Fig. 6).

## 2.3. *Docking study*

One of potential keys in cancer treatment is blocking of receptor tyrosine kinases (TKs) which are over expressed in cancer [38]. In this study, EGFR, was chosen as a biological target for carrying molecular modeling study for the newly synthesized compounds **5a–l**. Using Protein Data Bank (PDB: ID: 1M17), the crystal structure of EGFR

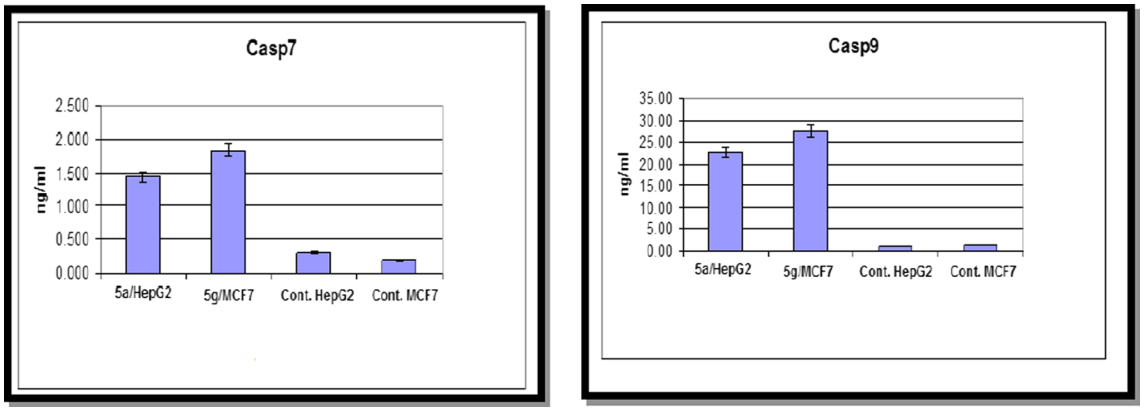


**Fig. 2.** Protein expression level of caspase-7 and caspase-9 in HepG2 and MCF-7 cell lines treated with compounds **5a** and **5g** against control untreated cells.

kinase with its inhibitor erlotinib (4-anilinoquinazoline) was obtained [39]. Molecular Operating Environment (MOE, Version 2005.06, Chemical Computing Group Inc., Montreal, Quebec, Canada) used for docking calculations. Erlotinib was docked first into the active site of EGFR and then the new compounds **5a–l** to compare their binding mode to that of erlotinib.

By inspecting the mode of binding of erlotinib, it was found that it interacts with Cys 773 amino acid *via* a hydrogen bond with its side chain oxygen atom and the docking score was −11.0797 Kcal/mol at 2.6 Å. The most active derivatives **5a** and **5g** against HepG2 and MCF7 cell lines showed one hydrogen bond between C═O of phthalimide part and the backbone amino acids Cys 773-the same as the reference erlotinib- or with Thr 830 with docking scores −15.6589 and −19.6074, respectively.

On the other side, rest of compounds containing carboxylic acid group in their structures bind to Lys 721 amino acid through a hydrogen bond with oxygen in COOH group rather than C═O of phthalimide core.

Some of active compounds (either on HepG2 and/or MCF7) didn't interact with any of amino acids inside the active site of EGFR enzyme. Specially those of unsubstituted phthalimide scaffold bearing CN or Cl groups at their phenyl spacer of benzoxazole and benzothiazole derivatives **5b**, **5c**, **5h** and **5i**. Their docking scores were in the range −17.4219 to −12.3223 Kcal/mol higher than that of erlotinib −11.0797 Kcal/mol.

Finally, we could conclude that hydrogen bonds between C═O group of phthalimide core might be important for activity. Moreover, hydrogen bonds with Cys 773 and Thr 830 backbone amino acids played an important role in fixation of compounds inside the enzyme active site led to increase in cytotoxic activity rather than Lys 721 amino acid and COOH group.

All the binding modes, interactions and docking scores are tabulated in S1 (supporting information), and pictured as in Figs. 7 and 8.

## 3. Conclusion

The newly synthesized benzoxazole/benzothiazole-phthalimide hybrids were evaluated for cytotoxic activity against two human cancerous cell lines, liver HepG2 and breast MCF7 cell lines, and non-cancerous fibroblast cells (WI-38) *in-vitro*. They possess potency against two cancer cell lines, HepG2 and MCF7. The most active compounds **5a** (on HepG2) and **5g** (on MCF7) were also able to activate caspase-7 and 9 enzymes led to induce apoptosis. Cell cycle analysis represented evidence through apoptosis of the HepG2 and MCF7 cancer cells at pre G1 and cell arrest at G2/M phase.

The prepared compounds had no cytotoxic activity on non cancerous cell line (WI-38) if compared with the used cancerous cell lines HepG2 and MCF7.

From the obtained results, we concluded that apoptosis was the mechanism for antiproliferative activity of the synthesized compounds rather than kinase inhibition against EGFR and HER2 enzymes. Benzoxazole derivative **5a** and its benzothiazole analogue **5g** possessed the highest potency against HepG2 and MCF7 cell lines with $IC_{50}$ = 0.011 and 0.006 μM, respectively. Similarly, they exerted the highest ability to activate caspase-7 and caspase-9 enzymes required for apoptosis. Subsequently, they arrested the cell cycle by 45.54% and 33.94%, sequentially at the G2/M stage. They showed high scores in molecular modeling study −15.65 and −19.60 and had one hydrogen

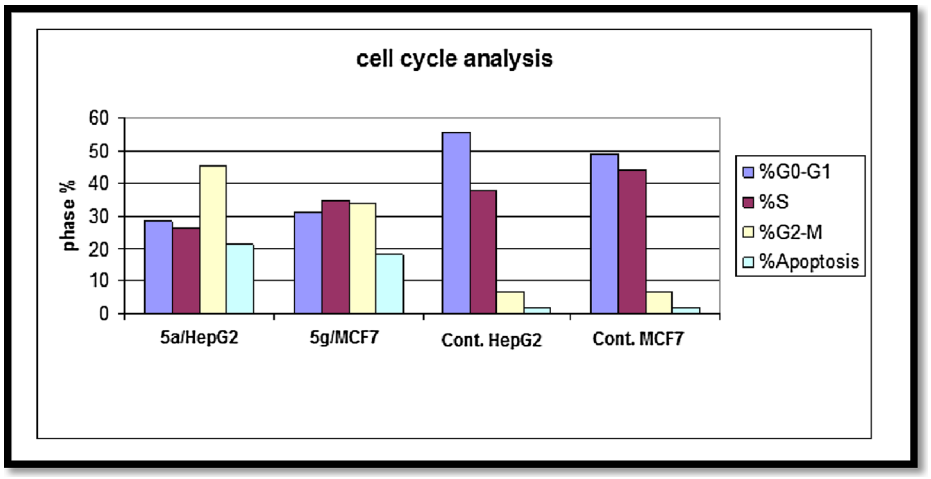


**Fig. 3.** Cell cycle analysis and apoptosis effect of compounds **5a** and **5g** on MCF7 and HepG2 cell lines.

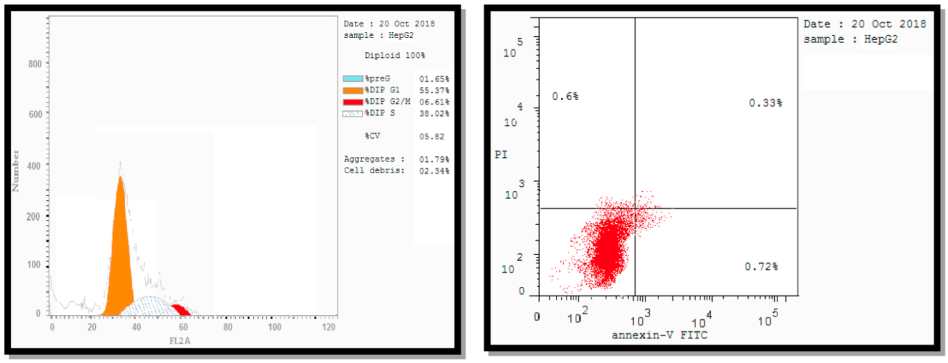


**Cont. HepG2**

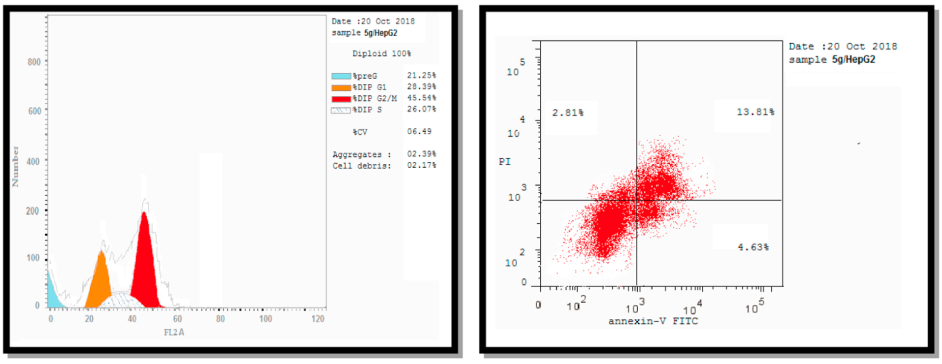


**5g/HepG2**

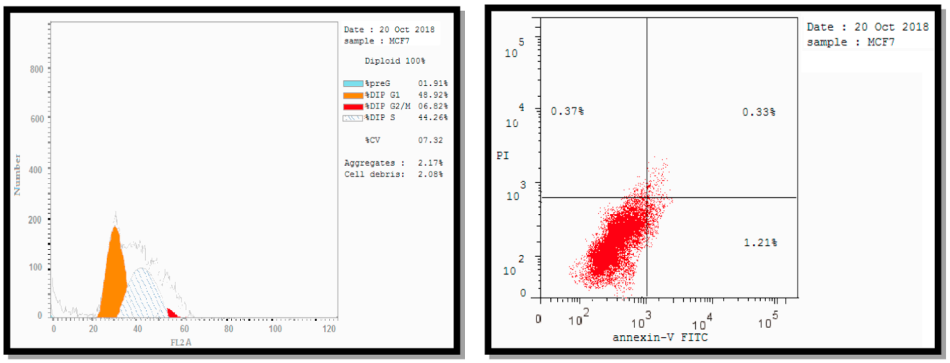


**Cont. MCF7**

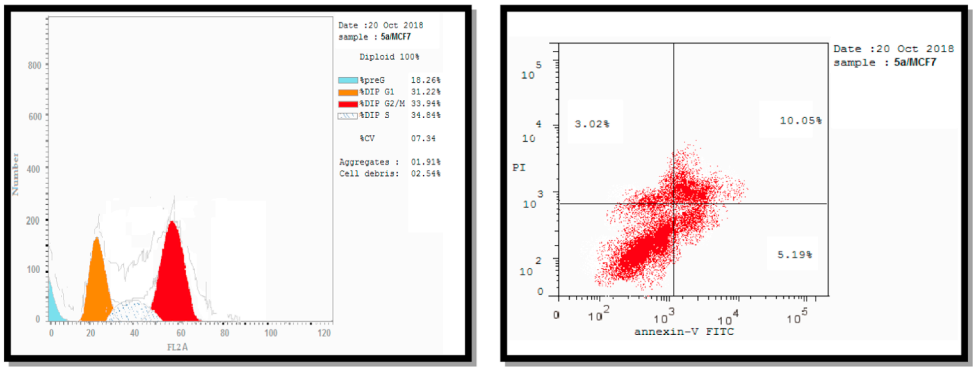


**5a/MCF-7**

**Fig. 4.** Cell cycle analysis using PI staining method by flow cytometry for **5a**, **5g**, control MCF7 and control HepG2.

**Table 4**
% apoptotic cell in case of treatment with compounds **5a** and **5g** on HepG2 and MCF7 cells, sequentially, against their control.

| Compound No. | Results | | | | Comment |
|---|---|---|---|---|---|
| | % G0-G1 | % S | % G2-M | % Pre-G1 | |
| **5a** | 28.39 | 26.07 | 45.54 | 21.25 | PreG1apoptosis, Cell growth arrestatG2/M. |
| **5g** | 31.22 | 34.84 | 33.94 | 18.26 | PreG1apoptosis, Cell growth arrestatG2/M. |
| **Control HepG2** | 55.37 | 38.02 | 6.61 | 1.65 | |
| **Control MCF-7** | 48.92 | 44.26 | 6.82 | 1.91 | |

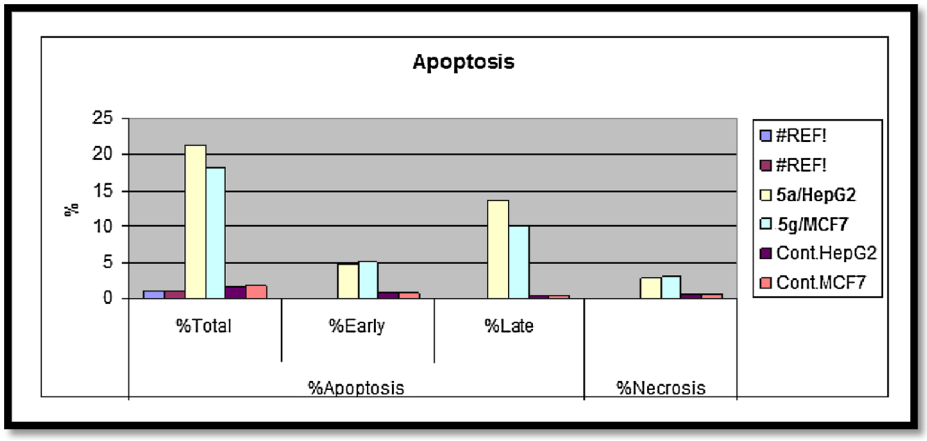


**Fig. 5.** Graphical representation of % apoptotic cell in case of treatment with compounds **6a** and **5g** on HepG2 and MCF7 cells, sequentially, against their control.

bond with Cys 773 and Thr 830 amino acids in EGFR active site, respectively.

## 4. Experimental

### 4.1. Chemistry

#### 4.1.1. General

Melting points were determined using a Griffin apparatus and are uncorrected. Infrared spectra (IR) were recorded, using KBr discs, on a Shimadzu IR-435 spectrophotometer and values were represented in $cm^{-1}$. $^{1}H$ NMR and $^{13}C$ NMR (DEPT-Q) were carried out using the Bruker instrument at 400 MHz for $^{1}H$ NMR and 100 MHz for $^{13}C$ NMR spectrophotometer, (Faculty of Pharmacy, Beni-Suef University, Beni-Suef, Egypt), in DMSO-$d_6$, $D_2O$ using TMS as an internal standard and chemical shifts were recorded in ppm on the $\delta$ scale using DMSO-$d_6$ (2.5) as a solvent. Coupling constant ($J$) values were estimated in Hertz (Hz). Splitting patterns are designated as follows: s, singlet; d, doublet, t, triplet; q, quartet; dd, doublet of doublet; m, multiplet. The electron impact (EI) mass spectra were recorded on a Hewlett Packard 5988 spectrometer (Palo Alto, CA). Microanalysis was performed for C, H, N on Perkin-Elmer 2400 at the Microanalytical center, Cairo University, Egypt and was within + 0.4% of theoretical values. Analytical thin layer chromatography (TLC): pre-coated plastic sheets, 0.2 mm silica gel with UV indicator (Macherey-Nagel) was employed routinely to follow the course of reactions and to check the purity of products. All other reagents, solvents were purchased from the Aldrich Chemical Company (Milwaukee, WI) and, were used without further purification. Benzoxazole **3a**, **3c** and benzothiazole derivatives **3f–i** were prepared according to literature procedures [14,33].

#### 4.1.2. General procedure for synthesis of compounds *3b* & *3d*

A mixture of 2-aminothiophenol **1a** (1.09 g, 0.01 mol) and 3-methyl-4-aminobenzoic acid **2b** or 3-chloro-4-aminobenzoic acid **2d** (0.01 mol) was heated in polyphosphoric acid (PPA; 85 g) at 220 °C for 4 h, cooled, then poured into ice-cold 10% aqueous sodium carbonate. The obtained solid was filtered, washed with water, and crystallized from 95% ethanol.

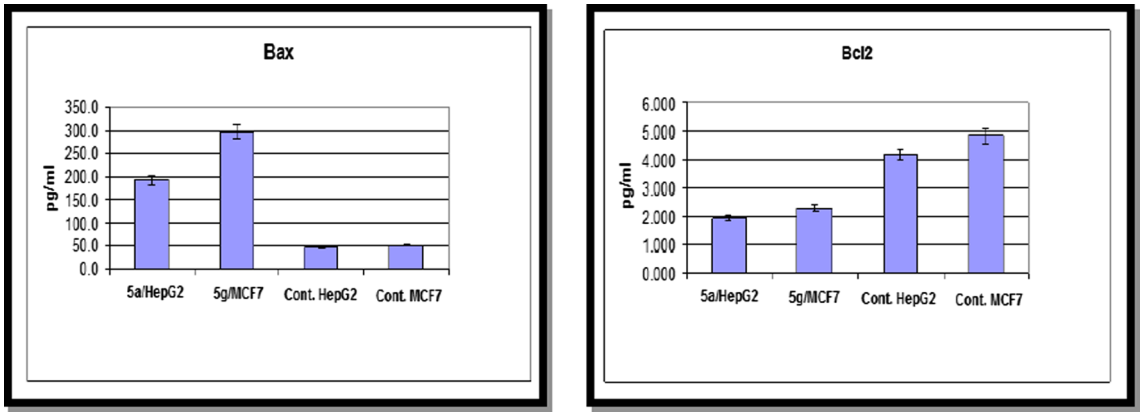


**Fig. 6.** Effect of compounds **5a** and **5g** on Bax and Bcl-2 expression levels.

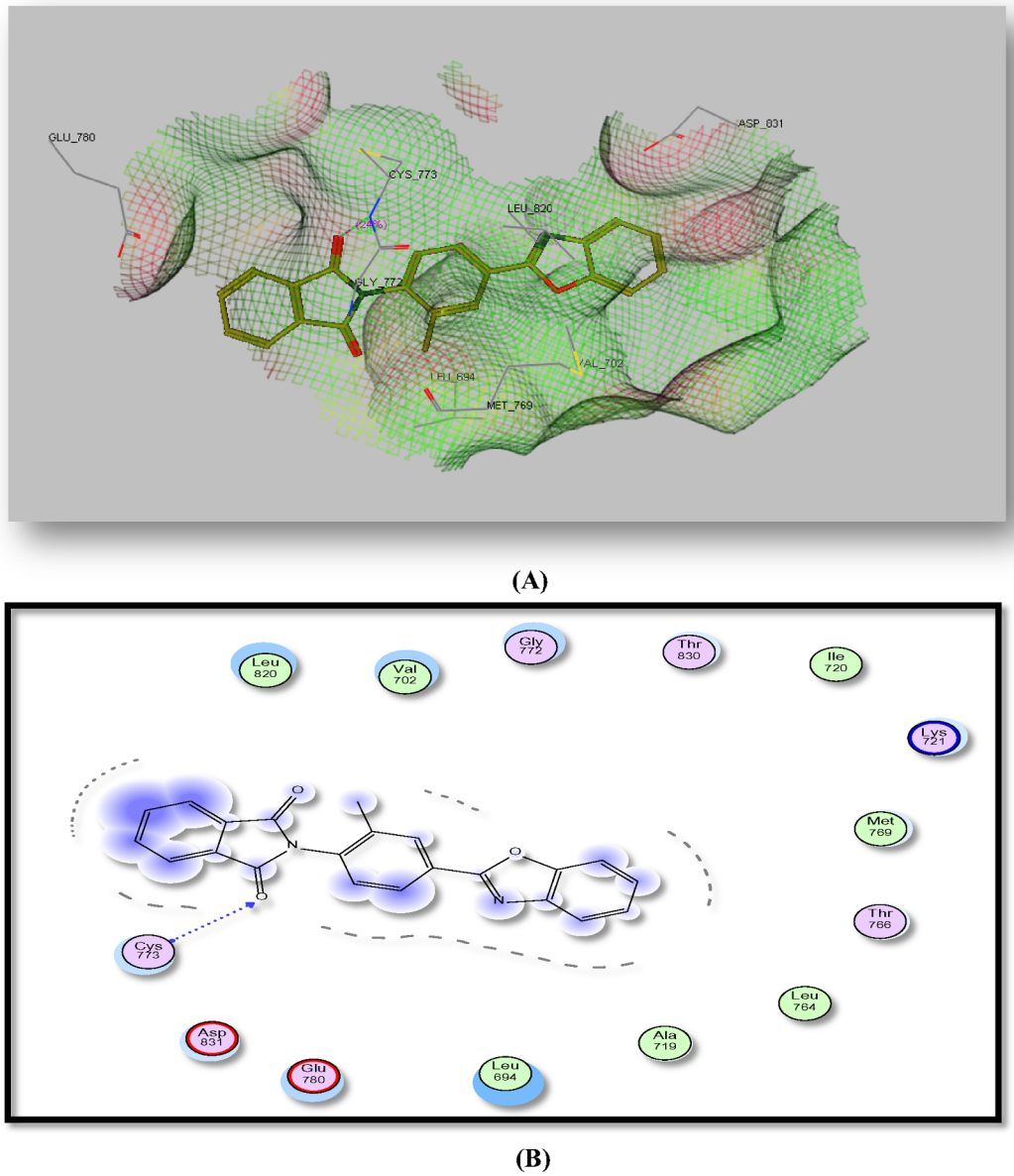


**Fig. 7.** (A) 3D interaction, (B) 2D interaction of compound **5a** inside EGFR active site.

*4.1.2.1. 4-(Benzo[d]oxazol-2-yl)-2-methylaniline (**3b**).* Buff solid; Yield 72%; m.p. 186–188 °C; IR (KBr) 3230,3117 ($NH_2$) $cm^{-1}$; $^1H$ NMR (DMSO-$d_6$, δ ppm) δ 2.12 (s, 3H, $CH_3$), 6.53 (s, 2H, $NH_2$, $D_2O$ exchangeable), 6.57 (d, $J$ = 7.5 Hz, 1H, aminophenyl H-5), 7.35 (d, $J$ = 7.5 Hz, 1H, aminophenyl H-6), 7.39–7.41 (m, 2H, benzoxazoleH-4, H-7), 7.54 (s, 1H, aminophenyl H-2), 7.74–7.83 (m, 2H, benzoxazole H-5, H-6); $^{13}C$ NMR (DMSO-$d_6$, δ ppm): 18.60 ($CH_3$), 110.46 (benzoxazoleC-7), 113.60 (aminophenyl C-5), 116.03 (aminophenyl C-1), 119.12 (benzoxazole C-4), 121.88 (aminophenyl C-3), 123.81 (benzoxazoleC-6), 124.18 (benzoxazoleC-5), 125.35 (aminophenyl C-6), 131.34 (aminophenyl C-2), 141.59 (benzoxazole C-3a), 150.68 (benzoxazole C-7a), 150.88 (aminophenyl C-4), 162.70 (benzoxazole C-2); Anal. Calcd for $C_{14}H_{12}N_2O$ (224.26): C, 74.98; H, 5.39; N, 12.49. Found: C, 74.96; H, 5.58; N, 12.42.

*4.1.2.2. 4-(Benzo[d]oxazol-2-yl)-2-chloroaniline (**3d**).* Creamy solid; Yield 76%; m.p. 155–157 °C; IR (KBr) 3232, 3120 ($NH_2$) $cm^{-1}$; $^1H$ NMR (DMSO-$d_6$, δ ppm) δ 6.49 (s, 2H, $NH_2$, $D_2O$ exchangeable), 6.63 (d, $J$ = 7.5 Hz, 1H, aminophenyl H-5), 7.39–7.41 (m, 2H, benzoxazoleH-4, H-7), 7.45 (d, $J$ = 7.5 Hz, 1H, aminophenyl H-6), 7.73–7.81 (m, 2H, benzoxazole H-5, H-6), 7.83 (s, 1H, aminophenyl H-2); $^{13}C$ NMR (DMSO-$d_6$, δ ppm): 110.34 (benzoxazoleC-7), 115.30 (aminophenyl C-5), 117.05 (aminophenyl C-3), 117.50 (aminophenyl C-1), 119.33 (benzoxazole C-4), 123.80 (benzoxazoleC-6), 124.15 (benzoxazoleC-5), 125.88 (aminophenyl C-5), 128.26 (aminophenyl C-2), 141.47 (benzoxazole C-3a), 147.71 (aminophenyl C-4), 150.09 (benzoxazole C-7a), 162.53 (benzoxazole C-2); Anal. Calcd for $C_{13}H_9ClN_2O$ (244.68): C, 63.81; H, 3.71; N, 11.45. Found: C, 63.75; H, 3.78; N, 11.43.

*4.1.3. General procedure for synthesis of compounds (**5a–l**)*

A mixture of benzoxazole or benzothiazole derivative **3a–i** (0.01 mol), and the appropriate phthalic anhydride derivative **4a&b** (0.01 mol), in glacial acetic acid (10 mL) was refluxed for 10–12 h. (monitored by TLC). The precipitated that formed after cooling or on hot (in case of benzothiazole derivatives) was filtered, dried and crystalized from a mixture of methanol/chloroform (2:1) to afford **5a–l**.

*4.1.3.1. 2-[4-(Benzo[d]oxazol-2-yl)-2-methylphenyl]isoindoline-1,3-dione (**5a**).* Brown solid; Yield 71%; m.p. 252–254 °C; IR (KBr) 1774, 1717

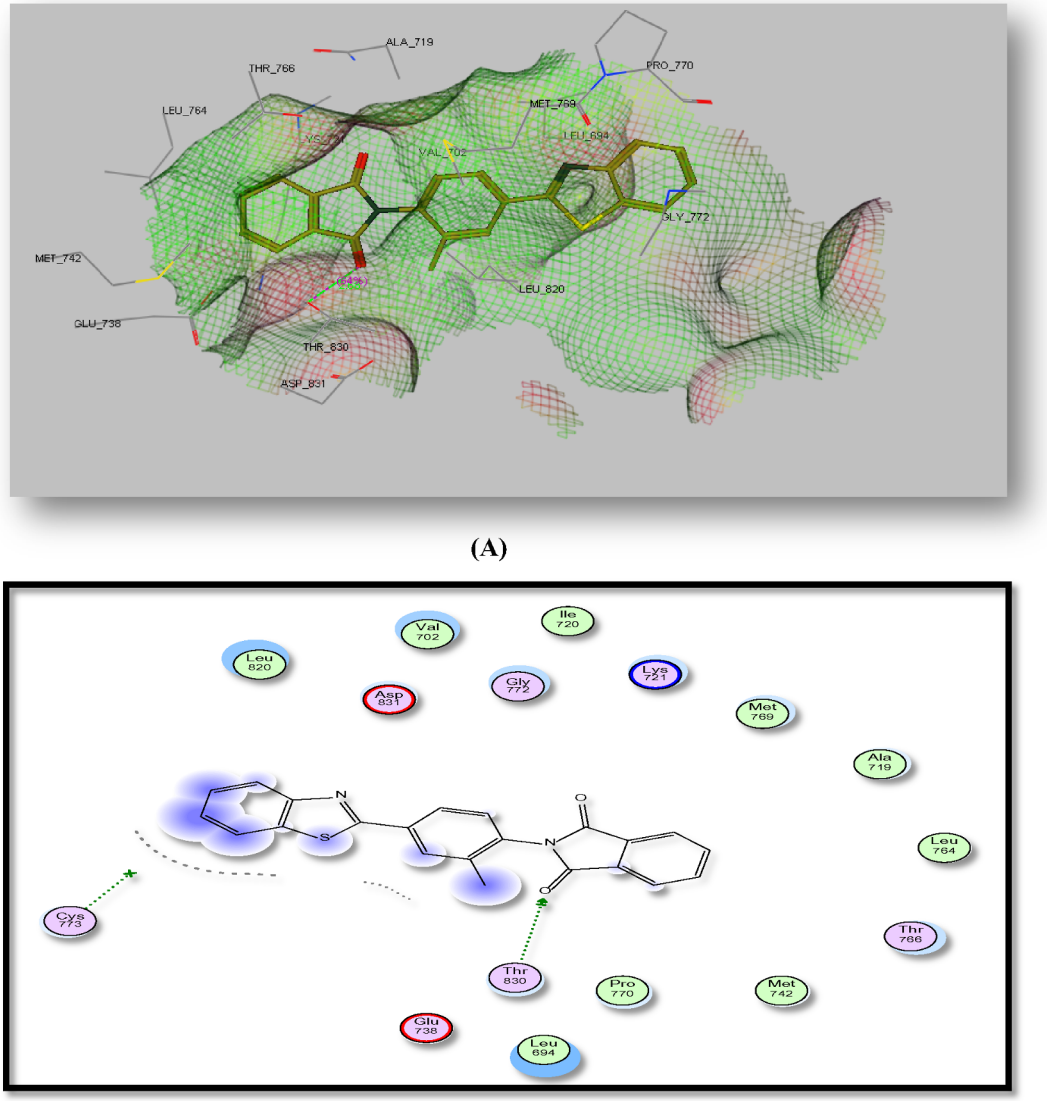


**Fig. 8.** (A) 3D interaction, (B) 2D interaction of compound **5g** inside EGFR active site.

(2C═O) $cm^{-1}$; $^1H$ NMR (DMSO-$d_6$, δ ppm) $\delta$2.26 (s, 3H, $CH_3$), 7.43–7.45 (m, 2H, benzoxazoleH-4, H-7), 7.68 (d, $J$ = 8 Hz, 1H, phenyl H-6), 7.78–7.83 (m, 2H, benzoxazole H-5, H-6),7.94–7.96 (m, 2H, isoindoline H-4, H-7), 8.01–8.03 (m, 2H, isoindoline H-5, H-6), 8.23 (d, $J$ = 8 Hz, 1H, phenyl H-5), 8.29 (s, 1H, phenyl H-3); $^{13}C$ NMR (DMSO-$d_6$, $\delta$ ppm): 18.20 ($CH_3$), 111.41 (benzoxazoleC-7), 120.32 (benzoxazole C-4), 124.07 (phenyl C-6), 125.48 (phenyl C-4), 125.52 (isoindoline C-4, C-7), 126.17 (benzoxazoleC-6), 128.18 (benzoxazoleC-5), 128.72 (phenyl C-5), 132.25 (isoindoline C-3a, C-7a), 132.35 (phenyl C-3), 135.25 (isoindolineC-5, C-6), 141.39 (benzoxazole C-3a), 141.88 (phenyl C-1), 150.66 (benzoxazole C-7a), 161.99 (benzoxazole C-2), 167.41 (isoindoline 2C═O); Anal. Calcd for $C_{22}H_{14}N_2O_3$ (354.36): C, 74.57; H, 3.98; N, 7.91. Found: C, 74.69; H, 3.85; N, 7.88.

*4.1.3.2. 5-(Benzo[d]oxazol-2-yl)-2-(1,3-dioxoisoindolin-2-yl)benzonitrile* ***(5b)***. Green solid; Yield 68%; m.p. 318–320 °C;IR (KBr) 2358 (C≡N), 1786, 1703 (2C═O) $cm^{-1}$; $^1H$ NMR (DMSO-$d_6$, δ ppm) $\delta$ 7.42–7.48 (m, 2H, benzoxazole H-4, H-7), 7.83–8.15 (m, 7H, benzoxazole H-5, H-6, dioxoisoindolin H-4, H-5, H-6, H-7 and benzonitrile H-5), 8.57 (d, 1H, $J$ = 7.6 Hz, benzonitrile H-3), 8.88 (s, 1H, benzonitrile H-6); $^{13}C$ NMR (DMSO-$d_6$, $\delta$ ppm): 111.57 (benzoxzoleC-7), 113.45 (phenyl C-1), 1116.21 (C≡N), 120.48 (benzoxazoleC-4), 121.20 (phenyl C-3), 123.10 (phenyl C-5), 124.63 (isoindoline C-4, C-7), 125.59 (benzoxazoleC-6), 126.36 (benzoxazole C-5), 126.88 (phenyl C-6), 131.81 (isoindoline C-3a, C-7a), 132.55 (phenyl C-4), 136.10 (isoindoline C-5, C-6), 141.12 (benzoxazole C-3a), 142.03 (phenyl C-2), 151.00 (benzoxazole C-7a), 165.80 (benzoxazole C-2), 166.31 (isoindoline 2C═O); Anal. Calcd for $C_{22}H_{11}N_3O_3$ (356.34): C, 72.33; H, 3.03; N, 11.50. Found: C, 72.57; H, 3.15; N, 11.48.

*4.1.3.3. 2-[(4-Benzo[d]oxazol-2-yl)-2-chlorophenyl]isoindoline-1,3-dione* ***(5c)***. Brown solid; Yield 73%; m.p. 260–262 °C;IR (KBr) 1776, 1720 (2C═O) $cm^{-1}$; $^1H$ NMR (DMSO-$d_6$, δ ppm) $\delta$ 7.43–7.50 (m, 2H, benzoxazole H-4, H-7), 7.80–7.86 (m, 2H, benzoxazole H-5, H-6), 7.97–8.06 (m, 5H, dioxoisoindolin H-4, H-5, H-6, H-7 and chlorophenyl H-6), 8.35 (d, 1H, $J$ = 8.4 Hz, chlorophenyl H-5), 8.55 (s, 1H, chlorophenylH-3); $^{13}C$ NMR (DMSO-$d_6$, $\delta$ ppm): 111.56 (benzoxazoleC-7), 120.56 (benzoxazoleC-4), 124.32 (chlorophenyl C-6), 125.68 (isoindolineC-4, C-7), 126.57 (benzoxazole C-6), 126.90 (chlorophenyl C-4), 129.94 (benzoxazoleC-5), 130.59 (chlorophenyl C-5), 131.19 (chlorophenyl C-2), 131.60 (chlorophenyl C-3), 131.98

(isoindoline C-3a, C-7a), 135.60 (isoindoline C-5, C-6), 136.34 (chlorophenyl C-1), 141.78 (benzoxazole C-3a), 150.79(benzoxazole C-7a), 161.03 (benzoxazole C-2), 166.73 (isoindoline 2C═O); Anal. Calcd for $C_{21}H_{11}ClN_2O_3$ (374.78): C, 67.30; H, 2.96; N, 7.47. Found: C, 67.51; H, 3.05; N, 7.43.

*4.1.3.4. 2-[4-(Benzo[d]oxazol-2-yl)phenyl]-1,3-dioxoindoline-5-carboxylic acid (**5d**)*. Buff solid; Yield 72%; m.p. 329–331 °C; IR (KBr) 3060–2550 (OH), 1784, 1723, 1687 (3C═O) $cm^{-1}$; $^1H$ NMR (DMSO-$d_6$, δ ppm) δ7.44–7.49 (m, 2H, benzoxazole H-4, H-7), 7.75 (d, 2H, $J$ = 8.8 Hz, phenyl H-2, H-6), 7.82–7.86 (m, 2H, benzoxazoleH-5, H-6), 8.12 (d, 1H, $J$ = 8 Hz, dioxoisoindolin H-7), 8.35 (d, 2H, $J$ = 8.8 Hz, phenyl H-3, H-5), 8.38 (s, 1H, dioxoisoindolin H-4), 8.44 (dd, 1H, $J$ = 1.2 Hz, $J$ = 8 Hz, dioxoisoindolin H-6), 13.80 (s, 1H, OH, $D_2O$ exchangeable); $^{13}C$ NMR (DMSO-$d_6$, δ ppm): 111.51 (benzoxzoleC-7), 120.41 (benzoxazoleC-4), 123.97 (isoindoline C-7), 124.44(benzoxazoleC-6), 125.51(benzoxazoleC-5), 126.25(isoindoline C-4), 128.17 (phenyl C-3, C-5), 128.30 (phenyl C-2, C-6), 131.94 (phenyl C-4), 132.47 (isoindolineC-3a), 135.24 (phenyl C-1), 135.29 (isoindoline C-5), 136.09 (isoindoline C-6), 137.09(isoindoline C-7a), 141.92 (benzoxazole C-3a), 150.78 (benzoxazoleC-7a), 162.13(benzoxazoleC-2), 166.29 (isoindoline 2C═O), 166.46 (isoindolineCOOH);MS (*m/z*, %): 384 (M, 11.30), 68 (100.00); Anal. Calcd for $C_{22}H_{12}N_2O_5$ (384.34): C, 68.75; H, 3.15; N, 7.29. Found: C, 68.55; H, 3.18; N, 7.13.

*4.1.3.5. 2-[4-(Benzo[d]oxazol-2-yl)-2-methylphenyl]-1,3-dioxoisoindoline-5-carboxylic acid (**5e**)*. Redish-brown solid; Yield 70%; m.p. 299–301 °C;IR (KBr) 3162 (broad band, OH), 1780, 1727, 1680 (3C═O) $cm^{-1}$; $^1H$ NMR (DMSO-$d_6$, δ ppm) δ 2.28 (s, 3H, $CH_3$), 7.37–7.47 (m, 2H, benzoxazole H-4, H-7), 7.68 (d, 1H, $J$ = 8 Hz, phenyl H-6), 7.78–7.82 (m, 2H, benzoxazole H-5, H-6), 8.13 (d, 1H, $J$ = 8 Hz, phenyl H-5), 8.24 (d, 1H, $J$ = 8 Hz, dioxoisoindolin H-7), 8.32 (s, 1H, phenyl H-3), 8.36 (s, 1H, dioxoisoindolin H-4), 8.45 (d, 1H, $J$ = 8 Hz, dioxoisoindolin H-6), 13.75 (s, 1H, OH, $D_2O$ exchangeable); $^{13}C$ NMR (DMSO-$d_6$, δ ppm): 18.17 ($CH_3$), 111.40 (benzoxazoleC-7), 120.31 (benzoxazoleC-4), 124.01 (phenyl C-6), 124.48 (isoindoline C-7), 125.52 (benzoxazoleC-6), 125.75 (benzoxazoleC-4), 126.19 (benzoxazole C-5), 128.29 (isoindoline C-4), 128.59 (phenyl C-5), 132.21 (isoindoline C-3a), 132.42 (phenyl C-3), 132.75 (isoindoline C-5), 135.56 (phenyl C-2), 136.02 (isoindoline C-6), 137.02 (phenyl C-1), 141.40 (isoindoline C-7a), 141.83 (benzoxazoleC-3a), 150.64 (benzoxazole C-7a), 161.95 (benzoxazole C-2), 166.35 (isoindoline 2C═O), 166.71 (isoindoline COOH); Anal. Calcd for $C_{23}H_{14}N_2O_5$ (398.37): C, 69.34; H, 3.54; N, 7.03. Found: C, 69.51; H, 3.48; N, 7.11.

*4.1.3.6. 2-[4-(Benzo[d]oxazol-2-yl)-2-chlorophenyl]-1,3-dioxoisoindoline-5-carboxylic acid (**5f**)*. Grey solid; Yield 73%; m.p. 286–288 °C;IR (KBr) 3273 (broad band OH), 1785, 1734, 1679 (3C═O) $cm^{-1}$; $^1H$ NMR (DMSO-$d_6$, δ ppm) δ 7.43–7.50 (m, 2H, benzoxazole H-4, H-7), 7.81–7.85 (m, 2H, benzoxazole H-5, H-6), 7.99 (d, 1H, $J$ = 8.4 Hz, chlorophenyl H-6), 8.17 (d, 1H, $J$ = 7.6 Hz, dioxoisoindolin H-7), 8.36 (d, 1H, $J$ = 8.4 Hz, chlorophenyl H-5), 8.39 (s, 1H, chlorophenyl H-3), 8.48 (d, 1H, $J$ = 7.6 Hz, dioxoisoindolin H-6), 8.57 (s, 1H, dioxoisoindolin H-4), 13.84 (s, 1H, OH, $D_2O$ exchangeable); $^{13}C$ NMR (DMSO-$d_6$, δ ppm): 111.57 (benzoxazoleC-7), 120.57 (benzoxazoleC-4), 124.26 (isoindoline C-7), 125.68 (benzoxazole C-6), 126.59 (benzoxazole C-5), 126.93 (chlorophenyl C-4), 130.05 (isoindoline C-4), 130.45 (chlorophenyl C-5), 130.96 (chlorophenyl C-2), 131.66 (chlorophenyl C-3), 132.42 (isoindoline C-3a), 135.18 (isoindoline C-5), 136.23 (chlorophenyl C-1), 136.36 (isoindoline C-6), 137.42 (isoindoline C-7a), 141.78 (benzoxazoleC-3a), 150.79 (benzoxazole C-7a), 160.99 (benzoxazoleC-2), 165.97 (isoindoline 2C═O), 166.20 (isoindolineCOOH); Anal. Calcd for $C_{22}H_{11}ClN_2O_5$ (418.79): C, 63.10; H, 2.65; N, 6.69. Found: C, 62.97; H, 2.72; N, 6.52.

*4.1.3.7. 2-[4-(Benzo[d]thiazol-2-yl)-2-methylphenyl]isoindoline-1,3-dione (**5g**)*. Green solid; Yield 77%; m.p. 260–262 °C;IR (KBr) 1779, 1709 (2C═O) $cm^{-1}$; $^1H$ NMR (DMSO-$d_6$, δ ppm) δ2.24 (s, 3H, $CH_3$), 7.48 (t, 1H, $J$ = 7.6 Hz, benzothiazole H-6), 7.56 (t, 1H, $J$ = 7.6 Hz, 1H, benzothiazoleH-5), 7.63 (d, 1H, $J$ = 8 Hz, phenyl H-6), 7.95–8.06 (m, 5H, isoindoline H-4, H-5, H-6, H-7 and phenyl H-5), 8.12–8.18 (m, 2H, benzothiazole H-4, H-7), 8.21 (s, 1H, phenyl H-3); $^{13}C$ NMR (DMSO-$d_6$, δ ppm): 18.07 ($CH_3$), 122.93 (benzothiazoleC-4), 123.31 (benzothiazoleC-6), 124.05 (phenyl C-6), 126.13 (isoindoline C-4, C-7), 127.25 (benzothiazoleC-6), 128.15 (benzothiazoleC-5), 128.46 (phenyl C-5), 132.05 (phenyl C-4), 132.26 (phenyl C-3), 132.28 (isoindoline C-3a, C-7a), 132.47 (phenyl C-2), 134.94(benzothiazole C-7a), 135.23 (isoindolineC-5, C-6), 140.64 (phenyl C-1), 153.92 (benzothiazole C-3a), 166.73 (benzothiazole C-2), 167.46 (isoindoline 2C═O); Anal. Calcd for $C_{22}H_{14}N_2O_2S$ (370.42): C, 71.33; H, 3.81; N, 7.56. Found: C, 71.27; H, 3.85; N, 7.47.

*4.1.3.8. 5-(Benzo[d]thiazol-2-yl)-2-(1,3-dioxoisoindolin-2-yl)benzonitrile (**5h**)*. Yellow solid; Yield 73%; m.p. 263–265 °C;IR (KBr) 2234 (C≡N), 1784, 1720 (2C═O) $cm^{-1}$; $^1H$ NMR (DMSO-$d_6$, δ ppm) δ 7.54 (t, 1H, $J$ = 7.6 Hz, benzothiazole H-6), 7.62 (t, 1H, $J$ = 7.2 Hz, benzothiazole H-5), 7.95–8.26 (m, 7H, dioxoisoindolin H-4, H-5, H-6, H-7, benzothiazole H-7 and benzonitrile H-5, H-6), 8.62 (d, 1H, $J$ = 1.2 Hz, 8.4 Hz, benzothiazoleH-4), 8.75 (s, 1H, benzonitrileH-3); $^{13}C$ NMR (DMSO-$d_6$, δ ppm): 113.34 (phenyl C-1), 116.10 (C≡N), 123.13 (benzothiazoleC-4), 123.80 (benzothiazole C-7a), 124.60 (phenyl C-3), 126.75 (isoindoline C-4, C-7), 127.56 (benzothiazole C-6), 131.56 (benzothiazole C-5), 131.72 (phenyl C-5), 132.30 (phenyl C-6), 133.06 (phenylC-4), 134.76 (isoindoline C-3a, C-7a), 135.89 (isoindoline C-5, C-6), 136.91 (benzothiazole C-7a), 141.89 (phenyl C-2), 154.00 (benzothiazole C-3a), 164.95 (benzothiazole C-2), 166.37 (isoindoline 2C═O);Anal. Calcd for $C_{22}H_{11}N_3O_2S$ (381.41): C, 69.28; H, 2.91; N, 11.02. Found: C, 69.39; H, 2.84; N, 10.95.

*4.1.3.9. 2-[4-(Benzo[d]thiazol-2-yl)-2-chlorophenyl]isoindoline-1,3-dione (**5i**)*. Green solid; Yield 77%; m.p. 263–265 °C;IR (KBr) 1781, 1712 (2C═O) $cm^{-1}$; $^1H$ NMR (DMSO-$d_6$, δ ppm) δ7.51 (t, 1H, $J$ = 7.6 Hz, benzothiazole H-6), 7.59 (t, 1H, $J$ = 6.8 Hz, benzothiazole H-5), 7.92–8.10 (m, 6H, benzothiazoleH-4, H-7 and dioxoisoindolin H-4, H-5, H-6, H-7), 8.21 (d, 1H, $J$ = 7.6 Hz, chlorophenyl H-6), 8.27 (d, 1H, $J$ = 7.6 Hz, chlorophenyl H-5), 8.48 (s, 1H, chlorophenylH-3); $^{13}C$ NMR (DMSO-$d_6$, δ ppm): 123.03 (benzothiazoleC-4), 123.56 (benzothiazoleC-7), 124.30 (chlorophenyl C-6), 126.49 (isoindolineC-4, C-7), 126.93 (chlorophenyl C-4), 127.45 (benzothiazoleC-6), 129.87 (benzothiazoleC-5), 130.33 (chlorophenyl C-5), 131.19 (chlorophenyl C-2), 131.47 (chlorophenyl C-3), 132.02 (isoindoline C-3a, C-7a), 133.28 (benzothiazole C-7a), 135.22 (chlorophenyl C-1), 135.58 (isoindoline C-5, C-6), 153.85(benzothiazole C-3a), 165.53 (benzothiazole C-2), 166.78 (isoindoline 2C═O); Anal. Calcd for $C_{21}H_{11}ClN_2O_2S$ (390.84): C, 64.53; H, 2.84; N, 7.17. Found: C, 64.48; H, 2.91; N, 7.06.

*4.1.3.10. 2-[4-(Benzo[d]thiazol-2-yl)phenyl]-1,3-dioxo isoindoline-5-carboxylic acid (**5j**)*. Green solid; Yield 85%; m.p. 339–341 °C;IR (KBr) 3053–2543 (OH), 1774, 1720, 1676 (3C═O) $cm^{-1}$; $^1H$ NMR (DMSO-$d_6$, δ ppm) δ 7.50 (t, 1H, $J$ = 6.8 Hz, benzothiazole H-6), 7.58 (t, 1H, $J$ = 7.6 Hz, benzothiazole H-5), 7.71 (d, 2H, $J$ = 8.4 Hz, phenyl H-2, H-6), 8.10–8.14 (m, 2H, benzothiazole H-4, H-7), 8.19 (d, 1H, $J$ = 7.6 Hz, dioxoisoindolin H-7), 8.27 (d, 2H, $J$ = 8.4 Hz, phenyl H-3, H-5), 8.34 (s, 1H, dioxoisoindolin H-4), 8.44 (dd, 1H, $J$ = 1.2, 7.6 Hz, dioxoisoindolin H-6), 13.77 (s, 1H, OH, $D_2O$ exchangeable); $^{13}C$ NMR (DMSO-$d_6$, δ ppm): 122.92 (benzothiazoleC-4), 123.48 (benzothiazoleC-7), 123.94 (isoindoline C-7), 124.41 (benzothiazoleC-6), 126.21 (benzothiazoleC-5), 127.26 (isoindoline C-4), 128.17 (phenyl C-3, C-5), 128.27 (phenyl C-2, C-6), 132.52 (phenyl C-4), 132.73 (isoindoline C-3a), 134.75 (phenyl C-1), 135.15 (isoindoline C-

5), 135.36 (benzothiazole C-7a), 136.05 (isoindoline C-6), 137.04 (isoindoline C-7a), 154.03 (benzothiazole C-3a), 166.28 (benzothiazole C-2), 166.49 (isoindoline 2C═O), 166.90 (isoindolineCOOH); Anal. Calcd for $C_{22}H_{12}N_2O_4S$ (400.41): C, 65.99; H, 3.02; N, 7.00. Found: C, 65.78; H, 3.11; N, 7.15.

*4.1.3.11. 2-[4-(Benzo[d]thiazol-2-yl)-2-methylphenyl]-1,3-dioxoisoindoline-5-carboxylic acid (**5k**).* Greyish-green solid; Yield 78%; m.p. 292–294 °C; IR (KBr) 3365–2606 (OH), 1779, 1716, 1661 (3C═O) $cm^{-1}$; $^1H$ NMR (DMSO-$d_6$, δ ppm) $\delta$ 2.25 (s, 3H, $CH_3$), 7.48 (t, 1H, $J$ = 7.6 Hz, benzothiazole H-6), 7.56 (t, 1H, $J$ = 7.2 Hz, benzothiazole H-5), 7.63 (d, 1H, $J$ = 8 Hz, phenyl H-6), 8.05 (d, 1H, $J$ = 8 Hz, phenyl H-5), 8.12–8.18 (m, 3H, benzothiazole H-4, H-7 and dioxoisoindolin H-7), 8.23 (s, 1H, phenyl H-3), 8.36 (s, 1H, dioxoisoindolin H-4), 8.45 (d, 1H, $J$ = 7.6 Hz, dioxoisoindolin H-6), 13.75 (s, 1H, OH, $D_2O$ exchangeable); $^{13}C$ NMR (DMSO-$d_6$, $\delta$ ppm): 18.05 ($CH_3$), 122.92 (benzothiazoleC-4), 123.30 (benzothiazoleC-7), 123.99 (phenyl C-6), 124.45 (isoindolineC-7), 126.14 (benzothiazoleC-6), 127.26 (benzothiazoleC-5), 128.27 (isoindolineC-4), 128.31 (phenyl C-5), 132.04 (phenyl C-4), 132.27 (isoindolineC-3a), 132.32 (phenyl C-3), 135.63 (phenyl C-2), 135.98 (isoindoline C-6), 136.94 (phenyl C-1), 140.63 (isoindoline C-7a), 153.90 (benzothiazole C-3a), 166.33 (benzothiazole C-2), 166.68 (isoindoline 2C═O), 166.73 (isoindoline COOH); Anal. Calcd for $C_{23}H_{14}N_2O_4S$ (414.43): C, 66.66; H, 3.40; N, 6.76. Found: C, 66.74; H, 3.45; N, 6.69.

*4.1.3.12. 2-[4-(Benzo[d]thiazol-2-yl)-2-chlorophenyl]-1,3-dioxoisoindoline-5-carboxylic acid (**5l**).* Grey solid; Yield 75%; m.p. 319–321 °C;IR (KBr) 3068–2556 (OH), 1783, 1725, 1680 (3C═O) $cm^{-1}$; $^1H$ NMR (DMSO-$d_6$, δ ppm) $\delta$ 7.51 (t, 1H,$J$ = 7.6 Hz,benzothiazole H-6), 7.59 (t, 1H,$J$ = 7.2 Hz,benzothiazole H-5), 7.93 (d, 1H,$J$ = 8.4 Hz, chlorophenyl H-6), 8.08 (d, 1H, $J$ = 8 Hz, benzothiazole H-4), 8.16 (d, 1H, $J$ = 8.4 Hz, chlorophenyl H-5), 8.20 (d, 1H, $J$ = 8 Hz, benzothiazole H-7), 8.27 (dd, 1H, $J$ = 2.00, 8.4 Hz, dioxoisoindolin H-6), 8.39 (s, 1H, chlorophenyl H-3), 8.47 (d, 1H, $J$ = 8.4 Hz, dioxoisoindolin H-7), 8.49 (d, 1H, $J$ = 2.00 Hz, dioxoisoindolin H-4), 13.86 (s, 1H, OH, $D_2O$ exchangeable); $^{13}C$ NMR (DMSO-$d_6$, $\delta$ppm): 123.07 (benzothiazoleC-4), 123.57 (benzothiazoleC-7), 124.21 (isoindoline C-7), 124.71 (chlorophenyl C-6), 126.46 (benzothiazoleC-6), 127.42 (benzothiazoleC-5), 129.95 (isoindoline C-4), 130.15 (chlorophenyl C-5), 130.94 (chlorophenyl C-4), 130.96 (chlorophenyl C-2), 131.49 (chlorophenyl C-3), 132.45 (isoindoline C-3a), 133.29 (isoindoline C-5), 135.22 (chlorophenyl C-1), 135.48 (benzothiazole C-7a), 136.29 (isoindoline C-6), 137.32 (isoindoline C-7a), 153.38 (benzothiazole C-3a), 165.47 (benzothiazole C-2), 165.98 (isoindoline 2C═O), 166.20 (isoindolineCOOH); Anal. Calcd for $C_{22}H_{11}ClN_2O_4S$ (434.85): C, 60.76; H, 2.55; N, 6.44. Found: C, 60.68; H, 2.47; N, 6.39.

### 4.2. Biological activity

#### 4.2.1. Materials and methods

In this study, two human cell lines, hepatic cancer (HepG2), breast cancer (MCF7) and non-cancerous fibroblast cells (WI-38) were supplied from American Type Cell Culture Collection (ATCC, Manassas, USA) and was maintained at VACSERA, Giza, Egypt. The reference anticancer drugs chosen in this study, against HepG2 and MCF7 cell lines were 5-fluorouracil (5-FU) and erlotinib, respectively. Cells were cultured using DMEM (Invitrogen/Life Technologies) supplemented with a mixture of 10% FBS (Hyclone), 10 ug/ml of insulin (Sigma), and 1% penicillin-streptomycin. All of the other used chemicals and reagents were obtained from Sigma, or Invitrogen. Cells were platedin a 96-well plate for 24 h before the MTT assay as followed (cells density 1.2–1.8 × 10,000 cells/well) in a volume of 100 µL then complete growth medium + 100 uL of the tested compound per well [40].

#### 4.2.2. Measurement of cytotoxic activity by MTT assay

MTT (3-(4.5-dimrthylthiazol-2-yl)-2,5-diphenyltetrazolium bromide) assay was used to determine the cytotoxic activity of the test compounds according to the reported method [40]. Cells were plated in 96-multiwell plate in DMEM containing 10% FBS (fetal bovine serum) for 24 h. Then DMSO was used as a vehicle for treatment of cells, test compounds and reference drugs for 48 h. After that, the media was replaced with 200 µL DMEM containing 0.5 mg/ml of MTT and were incubated for 2 h. Remove the supernatant and 200 µL of DMSO was used to dissolve formazans precipitate. Finally, the absorbance was determined at 570 nm by using a micro plate reader.

#### 4.2.3. In-vitro enzyme inhibitory assay

To investigate the mechanism of inhibition of EGFR and HER2 kinases, a cell-free assay was used according to the reported method [41]. Kit used for immune-assay was cloud clone SEA757Hu 96 Tests. 200 µM (EGFR) was used. A dose-response curve was obtained from the values resulted from the following equation: E (%) = E max/(1 + [I]/$ID_{50}$), where E (%) is the fraction of the enzyme activity measured in the presence of the inhibitor, E max is the activity in the absence of the inhibitor, [I] is the inhibitor concentration and $ID_{50}$ is the inhibitor concentration at which E (%) = 0.5 E max. then, for each experiment, mean values of two independent replicates were used for the interpolation.

#### 4.2.4. Caspase-7 and 9 activation assays

HepG2 and MCF-7 Cell lines, pretreated with compounds **5a** and **5g** respectively, were incubated in Lysis Buffer (conc. 5 × $10^6$ cells/ml.) at room temperature for 60 min with gentle shaking and then the extracts were transferred to microcentrifuge tubes and centrifuged.

Then, lysates were diluted over the range of the assay using Standard Diluent Buffer. After that, standards or samples were added to the appropriate micro ELISA plate wells pre-coated with antibodies specific to CASP7 or CASP9. Then a biotinylated detection antibody specific for CASP7 or a polyclonal detection antibody specific for CAS9, captured by the first antibody, was added to eachmicro plate well successively and incubated. Following incubation, the unbound detection antibody was removed during a wash step and Avidin-Horseradish Peroxidase (HRP) conjugate was added to each micro plate well to bind to the Detection Antibody. The mixture was incubated again and washed to remove the unbound HRB followed by addition of substrate solution reactive with HRP to the wells. A blue colored conjugate was appeared and its optical density was directly proportional to the amount of CAS7 or CAS9 present in the sample or standard. The enzyme-substrate reaction was terminated by addition of a sulphuric acid and the optical density (OD) was measured spectrophotometrically at a wavelength of 450 nm. CASP7 or CAS9 concentrations were determined in the samples by comparing the O.D. of the samples to the standard curve.

#### 4.2.5. Cell cycle analysis

Both HepG2 and MCF-7 cells were incubated for 24 h after seeding into six-well plates (density of 2 × $10^5$ cells per well). Fetal bovine serum (FBS, 10%) was added to RPMI 1640 and the cells were cultured in it at 37 °C and 5% $CO_2$. Then the medium was replaced with medium (final DMSO concentration, 1% v/v) containing compounds **5a** and **5g** (0.011 and 0.006 µM). Incubation continued for 24 h and 48 h. After that, the cell layer was trypsinized, washed with cold phosphate buffered saline (PBS) and fixed with 70% ethanol. PBS was used to rinse the fixed cells and then the DNA fluorochrome PI in a solution containing Triton X-100 and RNase were used as a staining solution for 15 min at 37 °C according the instruction manual. Then a FACS Caliber flow cytometer (Becton Dickinson & Co., Franklin Lakes, NJ) was used to analyze the samples. The number of cells analyzed for each sample was chosen to be 10,000 [42].

#### 4.2.6. Measurement of apoptosis using Annexin-V-FITC apoptosis detection kit

Cells were stained with Annexin V-fluorescein isothiocyanate (FITC) and counterstaining with propidium iodide (PI) using Annexin V-FITC/PI apoptosis detection kit to determine apoptosis. $2 \times 10^5$ Cells were exposed to compounds **5a** and **5g** (0.011 and 0.006 μM) for 24 h and 48 h. The trypsinized cells and washed twice with cold phosphate-buffered saline (PBS) and stained with 5 μL Annexin V-FITC and 5 μL PI in 1 × binding buffer for 15 min at 37 °C in the dark. Then, FACS Caliber flow cytometer (Becton Dickinson Biosciences & Co., Franklin Lakes, NJ) was used to analyze the samples. The number of analyzed cells for each sample was 10,000 [42].

#### 4.2.7. Evaluation of Bax and Bcl-2 expressions

The cell culture samples were suspended in Lysis Buffer to concentration5 × $10^6$ cells/ml and incubated at room temperature for 60 min with gentle shaking. Then the extracts were centrifuged and the cleared lysates were transferred to clean microfuge tubules. Moreover, lysates were diluted using Standard Diluent Buffer over the range of the assay. After that, standards or samples were added to the appropriate micro ELISA plate wells pre-coated with antibodies specific to Bax or Bcl-2 and were incubated at room temperature, on a microplate shaker at 100 rpm if available, for 2 h. The excess sample or standard were then washed out and specific biotinylated monoclonal antibodies were added and bound to Bax or Bcl-2 captured by the first antibodies. Following that, 100 μL of diluted Streptavidin conjugated to Horseradish peroxidase (HRP) was added to all wells, including the blank well sand the all wells were incubated at room temperature, on a microplate shaker at 100 rpm if available, for 1 h. HRP was bound to the biotinylated monoclonal Bax or Bcl-2 antibodies. Excess conjugate was washed out and substrate was added. After a short incubation, the enzyme reaction was stopped by addition of acid and the color generated was read at 450 nm. The measured optical density is directly proportional to the concentration of Bax or Bcl-2 in either standards or samples.

### 4.3. Statistical analysis

To analyze statistically data obtained, computerized Prism 5 program was used using one-way ANOVA test and Tukey's as post ANOVA for multiple comparison at $P \leq 0.05$. Representation of data was as mean ± SEM.

### 4.4. Docking study

The crystal structure of erlotinib inside EGFR active site (PDB: ID: 1 M17) was obtained from the protein data bank at Research Collaboration for Structural Bioinformatics (RSCB) Protein Database (PDB). Docking of the co-crystallized ligand was carried out to study the scoring energy(s), root mean standard deviation (RMSD) and amino acid interactions. RMSD was used to measure superposing for the lead compound to be 2.61 Å. Both London dG force and force field energy were used for docking study and refinement of the obtained results. 3D structure for the synthesized compounds were built by Molecular Operating Environment (MOE, Version 2005.06, Chemical Computing Group Inc., Montreal, Quebec, Canada) preparing them for starting the docking procedure. Moreover, 3D protonation of the built structures, conformational analysis, and selecting the least energetic conformer were applied using the same docking protocol used with ligand and test compounds. Amino acid interactions, number and lengths of the hydrogen bonds were determined.

## Declaration of Competing Interest

Authors have no conflict of interest to declare.

## Acknowledgments

Authors would like to thank all members of Pharmaceutical Organic Chemistry, Faculty of Pharmacy, Beni-Suef University for their great help and support during the whole work. Also, we gratefully acknowledge Dr. Esam Rashwan, Head of the confirmatory diagnostic unit VACSERA-EGYPT, for carrying out the cell cycle analysis, apoptosis biomarkers and *in- vitro* enzyme inhibitory assays

## Appendix A. Supplementary material

Supplementary data to this article can be found online at https://doi.org/10.1016/j.bioorg.2019.102978.

## References

[1] X. Pu, Z. Tian, W. Liang, S. Chang-Yan, H. Jing, Z. Ying-Lan, Y. Li, Novel benzothiazole, benzimidazole and benzoxazole derivatives as potential antitumor agents: synthesis and preliminary *in vitro* biological evaluation, Molecules 17 (2012) 873–883.
[2] M.Y. Amal, M. Ahmed, H.B. Mona, Y.E. Rasha, S.S. Ahmed, Synthesis and anticancer activity of novel benzimidazole and benzothiazole derivatives against HepG2 liver cancer cells, Med. Chem. 8 (2012) 151–162.
[3] X. Xilei, Y. Yu, Z. Ning, L. Gang, Benzothiazoles exhibit broad-spectrum antitumor activity: their potency, structureactivity and structure-metabolism relationships, Eur. J. Med. Chem. 76 (2014) 67–78.
[4] K. Melén, P. Keskinen, A. Lehtonen, I. Julkunen, Interferoninduced gene expression and signaling in human hepatoma cell lines, J. Hepatol. 33 (2000) 764–772.
[5] A. Stefania, W. Geoffrey, L.S. Erica, K. Hachemi, B. Rana, R.B. David, F.G.S. Malcolm, S.M. Charles, D.B. Tracey, D.W. Andrew, Synthesis and biological properties of benzothiazole, benzoxazole, and chromen-4-one analogues of the potent antitumor agent 2-(3,4-dimethoxyphenyl)-5-fluorobenzothiazole (PMX610, NSC 721648), J. Med. Chem. 51 (2008) 5135–5139.
[6] H. Ian, A.J. Sharon, B.V. Rao, D.W. Andrew, F.G.S. Malcolm, Antitumor benzothiazoles. synthesis and pharmaceutical properties of antitumor 2-(4-aminophenyl)benzothiazole amino acid prodrugs, J. Med. Chem. 45 (2002) 744–747.
[7] P.K. Jauhari, A. Bhavani, V. Subhash, S. Kiran, R. Prem, Synthesis of some novel 2-substituted benzoxazoles as anticancer, antifungal, and antimicrobial agents, Med. Chem. Res. 17 (2008) 412–424.
[8] A. Ruhi, S. Nadeem, Biological aspects of emerging benzothiazoles: a short review, J. Chem. 1–12 (2013).
[9] S. Xuan-Hong, W. Zhao, X. Yong, Y. Ting-Hong, D. Mei, X. You-Zhi, W. Yu-Quan, Y. Luo-Ting, Synthesis and biological evaluation of novel benzothiazole-2-thiol derivatives as potential anticancer agents, Molecules 17 (2012) 3933–3944.
[10] X. Yong, L. Qian, Z. Yongxia, Y. Tinghong, W. Ningyu, L. Guobo, S. Xuanhong, L. Yantong, S. Bin, Y. Tao, Z. Lifeng, W. Wenshuang, S. Xuejiao, X. Ying, W. Yuquan, Y. Luoting, SKLB316, a novel small-molecule inhibitor of cell-cycle progression, induces G2/M phase arrest and apoptosis in vitro and inhibits tumorgrowth in vivo., Can. Lett. 355 (2014) 297–309.
[11] A.A. Yaseen, H.A. Haitham, S. Bahjat, H.J. Ihsan, O.B. Mohammad, A.A. Najim, A. Tahsin, L. Paolo, B. Bernardetta, S. Tiziana, L. Roberta, Synthesis and in vitro antiproliferative activity of new benzothiazole derivatives, ARKIVOC, xv(2008) 225–238.
[12] M.H. Pourgholami, L. Woon, R. Almajd, J. Akhter, P. Bowery, D.L. Morris, *In vitro* and *in vivo* suppression of growth of hepatocellularcarcinoma cells by albendazole, Cancer Lett. 165 (2001) 43–49.
[13] H. Ian, C.Mei-Sze, L.B. Helen, T. Valentina, D.B. Tracey, D.W. Andrew, F.G.S. Malcolm, Antitumor benzothiazoles. Synthesis and in vitro biological properties of fluorinated 2-(4-aminophenyl)benzothiazoles, J. Med. Chem. 44 (2001) 1446–1455.
[14] D.F. Shi, T.D. Bradshaw, S. Wrigley, C.J. McCall, P. Lelieveld, I. Fichtner, M.F.G. Stevens, Antitumor benzothiazoles. Synthesis of 2-(4-aminophenyl)benzothiazoles and evaluation of their activities against breast cancer cell lines in vitro and in vivo, J. Med. Chem. 39 (1996) 3375–3384.
[15] T.D. Bradshaw, D.F. Shi, R.J. Schultz, K.D. Paull, L. Kelland, A. Wilson, H.H. Fiebig, S. Wrigley, M.F.G. Stevens, Influence of 2-(4-aminophenyl)benzothiazoles on the growth of human ovarian carcinoma cell lines *in vitro* and *in vivo*, Br. J. Cancer 78 (1998) 421–429.
[16] M.S. Chua, E. Kashiyama, T.D. Bradshaw, S.F. Stinson, E. Brantley, E.A. Sausville, M.F.G. Stevens, Role of CYP1A1 in modulation of antitumour properties of the novel agent 2-(4-amino-3-methylphenyl)benzothiazole (DF 203, NSC 674495) in human breast cancer cells, Cancer Res. 60 (2000) 5196–5203.
[17] L. CheeOnn, S. Marie, J.S. David, C.B. Michael, F.G.S. Malcolm, D.B. Tracey, *In vitro*, *in vivo*, and in silico analyses of the antitumor activity of 2-(4-amino-3-methylphenyl)-5-fluorobenzothiazoles, Mol. Cancer Ther. 3 (12) (2004) 1565–1575.
[18] A.A.-M. Abdel-Aziz, Novel and versatile methodology for synthesis of cyclic imides and evaluation of their cytotoxic, DNA binding, apoptotic inducing activities and molecular modeling study, Eur. Med. Chem. 42 (2007) 614–626.
[19] N. Shunmugam, M. Syamantak, S. Upendra, R. Saranya, K. Neeraj, C. Suvro, S. Bikram, Synthesis and anti-angiogenic activity of benzothiazole, benzimidazole containing phthalimide derivatives, Bioorg. Med. Chem. Lett. 23 (2013) 287–290.

[20] U. Sharma, P. Kumar, N. Kumar, B. Singh, Recent advances in the chemistry of phthalimide analogues and their therapeutic potential, Mini-Rev. Med. Chem. 10 (2010) 678–704.
[21] M.C. Patrícia, P.C. Marcilia, A.C. Adriana, M.T.C. Suellen, V.O.C. Marcos, B.O.F. Gevânio, A.V. Daniel, V.F.J. Francisco, C.L.L. Ana, O.M. Manoel, P. Claudia, M.P.F. Paulo, Improvement of *in vivo* anticancer and antiangiogenic potential of thalidomide derivatives, Chem.-Biol. Inter. 239 (2015) 174–183.
[22] X. Meng, D. Han, S. Zhang, W. Guo, R. Cui, Z. Li, Synthesis and anti-inflammatory activity of *N*-phthalimidomethyl 2,3-dideoxy- and 2,3-unsaturated glycosides, Carbohydr. Res. 342 (2007) 1169–1174.
[23] T. Noguchi, H. Fujimoto, H. Sano, H. Miyajima, Y. Hashimoto, Angiogenesis inhibitors derived from thalidomide, Bioorg. Med. Chem. Lett. 15 (2005) 5509–5513.
[24] H. Sano, T. Noguchi, A. Miyajima, Y. Hashimoto, H. Miyachi, Anti-angiogenic activity of basic-type, selective cyclooxygenase (COX)-1 inhibitors, Bioorg. Med. Chem. Lett. 16 (2006) 3068–3072.
[25] S.H.L. Kok, R. Gambari, C.H. Chui, M.C.W. Yuen, E. Lin, R.S.M. Wong, F.Y. Lau, G.Y.M. Cheng, W.S. Lam, S.H. Chan, K.H. Lam, C.H. Cheng, P.B.S. Lai, M.W.Y. Yu, F. Cheung, J.C.O. Tang, A.S.C. Chan, Synthesis and anti-cancer activity of benzothiazole containing phthalimide on human carcinoma cell lines, Bioorg. Med. Chem. 16 (2008) 3626–3631.
[26] S.H. Chan, K.H. Lam, C.H. Chui, R. Gambari, M.C.W. Yuen, R.S.M. Wong, G.Y.M. Cheng, F.Y.L. Lau, Y.K. Au, C.H. Cheng, P.B.S. Lai, C.W. Kan, S.H.L. Lung-Kok, J.C.O. Tang, A.S.C. Chan, The preparation and *in vitro*antiproliferative activity of phthalimide based ketones on MDAMB-231 and SKHep-1 human carcinoma cell lines, Eur. J. Med. Chem. 44 (2009) 2736–2740.
[27] K.M. Cook, W.D. Figg, Angiogenesis inhibitors – current strategies and future prospects, CA Cancer J. Clin. 60 (2010) 222–243.
[28] M. Melchert, A. List, The thalidomide saga, Int. J. Biochem. Cell Biol. 39 (2007) 1489–1499.
[29] C.I. Chen, Lenalidomide alone and in combination for chronic lymphocytic leukemia, Curr. Hematol. Malig. Rep. 8 (2013) 7–13.
[30] C.B. Yeh, C.J. Su, J.M. Hwang, M.C. Chou, Therapeutic effects of cantharidin analogues without bridging ether oxygen on human hepatocellular carcinoma cells, Eur. J. Med. Chem. 45 (2010) 3981.
[31] F.L. Phoebe, Synthesis and antitumor activity of novel pyrazolo[3,4-*d*]pyrimidine and their tricyclic derivatives, Int. J. Pharm. Sci. Rev. Res. 24 (2) (2014) 208–214.
[32] M.K. Manal, M.R. Sameha, K.A.A. Eman, A.A. Mohamed, F.L. Phoebe, Design, synthesis and cytotoxic activity of some novel compounds containing pyrazolo[3,4-*d*]pyrimidine nucleus, J. Chem. Sci. 125 (5) (2013) 1029–1043.
[33] M.K. Manal, K.A.A. Eman, K.A. Mohammed, A.A. Mohamed, N.P. John, Synthesis and *in vitro* antitumor activity of new benzothiazole and benzoxazole derivatives, J. Chem. Pharm. Res. 5 (8) (2013) 16–21.
[34] K.A.A. Eman, N.P. John, Synthesis and cytotoxic activity of new pyrazolo[1,5-a] pyrimidinesand determination of pyrimidine regiospecific ring formation with 2D NMR, ARKIVOC, (v) (2016) 210–224.
[35] B.L. Madlen, F.L. Phoebe, Design, synthesis and biological evaluation of novel thiophene and theinopyrimidine derivatives as anticancer agents, Med. Chem. Res. 25 (11) (2016) 2607–2618.
[36] H.R. Stennicke, G.S. Salvesen, Catalytic properties of the caspases, Cell Death Differ. 6 (1999) 1054–1059.
[37] M.T. El Sayed, A.H. Nehal, A.O. Dalia, M.A. Khadiga, Indoles as anti-cancer agents, Adv. Mod. Oncol. Res. 1 (1) (2015) 20–35.
[38] S. Ghavami, M. Hashemi, S.R. Ande, B. Yeganeh, W. Xiao, M. Eshraghi, C.J. Bus, K. Kadkhoda, E. Wiechec, A.J. Halayko, M. Los, Apoptosis and cancer: mutations withincaspasegenes, J. Med. Genet. 46 (2009) 497.
[39] http://www.rcsb.org/pdb/explore/explore.do?structureId=1M17.
[40] J.M. Edmondson, L.S. Armstrong, A.O. Martinez, Manual of microbiologic monitoring of laboratory animals, J. Tiss. Cult. Meth. 11 (1988) 5.
[41] F. Manetti, G.A. Locatelli, G. Maga, S. Schenone, M. Modugno, S. Forli, F. Corell, M. Botta, Frontiers in drug design and discovery, J. Med. Chem. 49 (2006) 3278.
[42] K.K. Lo, T.K. Lee, J.S. Lau, W.L. Poon, S.H. Cheng, Luminescent biological probes derived from ruthenium (II) estradiol polypyridine complexes, Inorg. Chem. 47 (1) (2008) 200–208.